Copy No. 3

RM SA9J07

[redacted]

NACA

RESEARCH MEMORANDUM

for the

Air Materiel Command, U. S. Air Force

AERODYNAMIC CHARACTERISTICS OF AN 0.08-SCALE MODEL OF THE MARTIN XB-51 AIRPLANE AT HIGH SUBSONIC SPEEDS

By Robert H. Barnes

Ames Aeronautical Laboratory
Moffett Field, Calif.

CLASSIFIED DOCUMENT

This document contains classified information affecting the National Defense of the United States within the meaning of the Espionage Act, USC 50:31 and 32. Its transmission or the revelation of its contents in any manner to an unauthorized person is prohibited by law. Information so classified may be imparted only to persons in the military and naval services of the United States, appropriate civilian officers and employees of the Federal Government who have a legitimate interest therein, and to United States citizens of known loyalty and discretion who of necessity must be informed thereof.

NATIONAL ADVISORY COMMITTEE FOR AERONAUTICS

WASHINGTON

Oct. 7, 1949

[redacted]

NACA RM SA9J07

NATIONAL ADVISORY COMMITTEE FOR AERONAUTICS

RESEARCH MEMORANDUM

for the

Air Materiel Command, U. S. Air Force

AERODYNAMIC CHARACTERISTICS OF AN 0.08-SCALE MODEL OF THE MARTIN XB-51 AIRPLANE AT HIGH SUBSONIC SPEEDS

By Robert H. Barnes

SUMMARY

High-speed wind-tunnel tests were conducted of an 0.08-scale model of the XB-51 airplane for the purpose of determining force, stability, and control characteristics in pitch and yaw. The results indicate no adverse longitudinal characteristics up to a Mach number of 0.85. At higher Mach numbers the test results indicate unstable variations of elevator deflection and hinge moment with Mach number. The lateral and directional stability remained positive throughout the Mach number range of the tests.

INTRODUCTION

At the request of the Air Materiel Command, U. S. Air Force, tests were made of an 0.08-scale model of the Martin XB-51 airplane. The purpose of the tests was to determine the force, stability, and control characteristics in both pitch and yaw at high subsonic speeds.

NOTATION

The coefficients and symbols used in this report are defined as follows:

C_D drag coefficient $\left(\frac{\text{drag}}{qS}\right)$

C_L lift coefficient $\left(\frac{\text{lift}}{qS}\right)$

C_Y side-force coefficient $\left(\frac{\text{side force}}{qS}\right)$

C_h hinge-moment coefficient $\left(\frac{\text{hinge moment}}{2qM_A}\right)$

C_l rolling-moment coefficient $\left(\frac{\text{rolling moment}}{qSb}\right)$

C_m pitching-moment coefficient $\left(\frac{\text{pitching moment}}{qS\bar{c}}\right)$

C_n yawing-moment coefficient $\left(\frac{\text{yawing moment}}{qSb}\right)$

M Mach number

M_A moment about hinge line of control-surface area behind the hinge line, feet cubed

S wing area, square feet

V velocity, feet per second

b wing span, feet

c local wing chord, feet

$\bar{c}$ wing mean aerodynamic chord $\left(\frac{\int_0^{b/2} c^2\,dy}{\int_0^{b/2} c\,dy}\right)$, feet

i incidence, degrees

q dynamic pressure $\left(\frac{1}{2}\rho V^2\right)$, pounds per square foot

y lateral coordinate, measured from plane of symmetry, feet

α angle of attack, degrees

δ control-surface deflection, degrees

ρ free-stream mass density, slugs per cubic foot

ψ angle of yaw, degrees

$dC_n/d\psi$ slope of curve of yawing-moment coefficient versus angle of yaw measured at zero yaw, per degree

$dC_l/d\psi$ slope of curve of rolling-moment coefficient versus angle of yaw measured at zero yaw, per degree

$dC_Y/d\psi$ slope of curve of side-force coefficient versus angle of yaw measured at zero yaw, per degree

[redacted]

$dC_{h_r}/d\delta_r$ slope of curve of rudder hinge-moment coefficient versus rudder deflection measured at zero yaw and zero rudder deflection, per degree

$dC_{h_r}/d\psi$ slope of curve of rudder hinge-moment coefficient versus angle of yaw measured at zero yaw and zero rudder deflection, per degree

Subscripts

e elevator

r rudder

t horizontal tail

MODEL AND APPARATUS

The XB-51 is a high-speed light bomber for the U. S. Air Force. It has a swept-back wing and swept-back empennage and is powered by three turbojet engines, two being housed in nacelles mounted under the fuselage and one in the rear part of the fuselage. Normal cruising operation is to be with the two nacelle jet engines. This is the configuration which was simulated in the wind-tunnel tests. A three-view drawing of the model is presented in figure 1. In order to mount the model on the sting support it was necessary to modify the lines of the fuselage. The extent of these modifications is indicated in the figure. Photographs of the model mounted on the sting are shown in figure 2. Dimensional data are given in table I.

The model elevators and rudder were movable and equipped with strain gages for measuring hinge moments. The dive brakes as shown in their true shape in figure 1 were simple bent plates screwed to the fuselage.

The tests were conducted in the Ames 16-foot high-speed wind tunnel with the model mounted on a sting-support system. The sting was moved in such a manner that the model rotated about a point in space which corresponded closely to the reference center-of-gravity position shown in figure 1. For tests in yaw the model was rotated 90°, hence pitch movement became yawing movement. All yaw tests were conducted at an angle of attack of 0°.

Forces were measured by means of a four-component strain-gage balance mounted on the end of the sting support. The balance was housed within the fuselage of the model. For pitch tests the balance measured normal and chord forces and pitching and rolling moments. For yaw tests the balance measured chord and side forces and yawing and rolling moments.

With a few exceptions the tests were made over a Mach number range of 0.3 to 0.9, inclusive. The Reynolds number range was 1.7 to 3.7 million.

PRESENTATION OF DATA

Reduction of Data and Corrections

The forces as measured by the balance during pitch tests were resolved to give forces about the wind axes (i.e., lift and drag). Then the usual procedures were employed to transfer the forces and moments to the reference center-of-gravity position ($0.25\bar{c}$) and to reduce them to coefficient form. The force and moment coefficients for yaw tests were expressed about the model axes.

Wind-tunnel-wall corrections and constriction corrections were applied by the methods of references 1 and 2, respectively.

No corrections were made for the effect of the sting.

Order of Presentation of Data

The data for the model in pitch are presented in figures 3 to 9, inclusive. Included are the calculated variations with Mach number of elevator deflection and hinge moment for level flight.

The characteristics of the model in yaw are presented in figures 10 to 12.

The effects of dive brakes and of the bomb bay are presented in figures 13 and 14.

RESULTS AND DISCUSSION

Longitudinal Characteristics

Figure 6 shows that there was a slow increase of the lift-curve slope with Mach number up to a Mach number of 0.7. At larger Mach numbers the slope became increasingly greater, reaching a value of 0.11 per degree at a Mach number of 0.9 as contrasted with a value of 0.08 at 0.3 Mach number. It can be seen from figure 3 that the angle of attack for zero lift decreased roughly $1/2^\circ$ over the Mach number range of the tests. From figure 6 it can be seen that the Mach number of divergence for the drag ($\partial C_D/\partial M = 0.10$) was about 0.84 at zero lift and 0.85 at a lift coefficient of 0.2.

Figure 7 shows a gradual increase in the pitching-moment coefficient at constant lift coefficient as the Mach number was increased to about

[redacted]

0.85. This Mach number corresponds approximately to the design maximum speed in level flight for the airplane. The static stick-fixed longitudinal stability underwent only minor changes throughout the Mach number range of the tests. It is seen that the nacelles had a destabilizing effect. The horizontal tail effectiveness increased with Mach number up to a Mach number of about 0.875 and then decreased rather abruptly as the Mach number was increased to 0.90.

Figure 8 shows that the slope of the elevator hinge-moment curve $dC_{h_e}/d\delta_e$ was practically constant at -0.005 up to 0.85 Mach number. At 0.9 Mach number it had increased to a value of -0.007. This figure also shows that the elevator effectiveness increased from -0.0120 at 0.3 Mach number to -0.0146 at 0.85 Mach number. At 0.9 Mach number it returned to its low-speed value of -0.0120.

In figure 9 the variation with Mach number of the elevator angle for balance ($C_m = 0$) and the corresponding total hinge moment (2 elevators) are presented. Level flight is assumed at the various altitudes noted. The wing loading was 80.9 pounds per square foot and the center of gravity was at $0.25\bar{c}$. Elevator hinge moments are not shown for Mach numbers less than 0.6 since hinge-moment data were not taken at the large elevator angles required at 0.3 Mach number, the next lowest test Mach number.

The results indicate that the airplane will have both stick-fixed and stick-free stability up to a Mach number of 0.85. At greater Mach numbers both types of stability will become negative. However, even at 0.9 Mach number the elevator deflections and hinge moments are smaller than the maximums at 0.85 Mach number.

Lateral and Directional Characteristics

The variations of lateral and directional characteristics with Mach number as presented in figure 10 show no severe changes except in the dihedral effect $dC_l/d\psi$. With regard to this parameter it should be noted that, although the nacelles were below the center of gravity, their effect on $dC_l/d\psi$ had the same sign (positive) as the effect of the empennage which was above the center of gravity. The effect of the nacelles on $dC_Y/d\psi$ was what would be expected (i.e., positive side force at positive yaw) and their effect on $dC_n/d\psi$ was small. Therefore there is no apparent explanation for their effect on $dC_l/d\psi$.

In figure 11 typical variations of the rudder hinge-moment coefficient with angle of yaw and with rudder deflection are presented. In figure 12 the variations of $dC_{h_r}/d\psi$ and $dC_{h_r}/d\delta_r$ with Mach number are presented. At Mach numbers greater than 0.8 the variation of rudder hinge-moment coefficient with angle of yaw became positive for small angles of yaw. On the other hand, the variation of rudder hinge-moment

coefficient with rudder angle remained negative for small rudder angles throughout the Mach number range of the tests, indicating that there was no overbalancing of the rudder.

Effects of Dive Brakes and Bomb Bay

The effects of the dive brakes tested are shown in figure 13 in terms of incremental drag and pitching-moment coefficients at zero lift coefficient. The incremental drag data show that for a deflection of 30° the front drag brakes were the more effective. The incremental drags per unit area also were greater for the front dive brakes.

The incremental pitching-moment coefficients shown in figure 13 would require less than 0.5° of elevator deflection for correction. (See fig. 8.)

The effects of opening the bomb bay are shown in figure 14. Since the airplane is to have a revolving-type bomb bay carrying four 500-pound bombs, tests were made with the bomb bay half open (90° rotation) and fully open. Again, the results are presented as increments of drag and pitching-moment coefficients. All increments are taken at lift coefficients for level flight at 10,000 feet altitude at the various Mach numbers. The increments for the corresponding flight conditions at other altitudes would not be significantly different inasmuch as they are nearly constant at various lift coefficients.

The results show that at Mach numbers above 0.61 the effects of the half-open bomb bay were greater than for the fully open bay. At 0.8 Mach number the ratio of the effects was more than two to one. The maximum pitching-moment increment would require about 1.3° of elevator deflection for correction.

CONCLUSIONS

The results of the tests reported herein indicate that:

1. Up to a Mach number of 0.85 there were no adverse effects of compressibility on the longitudinal-stability and-control characteristics. At Mach numbers between 0.85 and 0.9 the adverse effects were not serious and should not introduce any stability and control problems.

2. At Mach numbers greater than 0.7 the static lateral and static directional stability decreased. However, up to the limit of the tests the model characteristics indicated stability.

3. At Mach numbers greater than 0.8 the variation of rudder hinge-moment coefficient with angle of yaw became positive. The variation of

the hinge-moment coefficient with rudder angle, however, remained negative for small rudder angles throughout the Mach number range tested.

4. The forward location of the fuselage dive brakes gave more drag.

5. At Mach numbers greater than 0.61 the half-open bomb bay had greater effects on both the drag and pitching-moment coefficients than the fully open bomb bay.

Ames Aeronautical Laboratory,
National Advisory Committee for Aeronautics,
Moffett Field, Calif.

REFERENCES

1. Silverstein, Abe, and White, James A.: Wind-Tunnel Interference with Particular Reference to Off-Center Positions of the Wing and to the Downwash at the Tail. NACA Rep. 547, 1935.

2. Herriot, John G.: Blockage Corrections for Three-Dimensional-Flow Closed-Throat Wind Tunnels with Consideration of the Effect of Compressibility. NACA RM A7B28, 1947.

TABLE I.- DIMENSIONS OF THE 0.08-SCALE MODEL OF THE XB-51 AIRPLANE

Wing	
Section	NACA 63A010
Area, square feet	3.52
Aspect ratio	5.16
Taper ratio	0.49
Vertical Tail	
Section	NACA 63A010
Area, square feet	0.475
Aspect ratio	1.0
Taper ratio	0.667
Rudder chord	0.20 vertical tail chord
Horizontal Tail	
Section	NACA 63A009
Area, square feet	0.694
Aspect ratio	4.1
Taper ratio	0.49
Elevator chord	0.20 horizontal tail chord
Fuselage	
Frontal area, square feet	0.298
Fineness ratio	11.8
Nacelle	
Frontal area (one), square feet	0.056
Diameter, inches	3.2
Fineness ratio	5.79
Nacelle Pylon	
Section	NACA 0006-64
Fuselage Dive Brakes	
True area behind hinge line (one brake)	
Front dive brake, square feet	0.051
Rear dive brake, square feet	0.032

FIGURE LEGENDS

Figure 1.– Three-view drawing of 0.08-scale model of the Martin XB-51 airplane.

Figure 2.– The 0.08-scale model of the XB-51 airplane mounted in the wind tunnel. (a) Lower front view. (b) Three-quarter front view.

Figure 3.– Variation of lift coefficient with angle of attack at various Mach numbers.

Figure 4.– Variation of lift coefficient with drag coefficient at various Mach numbers.

Figure 5.– Variation of lift coefficient with pitching-moment coefficient at various Mach numbers.

Figure 6.– Variation of lift-curve slope and drag coefficient with Mach number.

Figure 7.– Variation with Mach number of the pitching-moment coefficient, static longitudinal stability, and horizontal tail effectiveness.

Figure 8.– Variation of elevator hinge-moment slope and effectiveness with Mach number.

Figure 9.– Variation with Mach number of elevator angle and hinge moment at balance in level flight.

Figure 10.– Variation with Mach number of the lateral and directional characteristics.

Figure 11.– Typical variations of rudder hinge-moment coefficient with angle of yaw and with rudder angle.

Figure 12.– Variation of rudder hinge-moment characteristics with Mach number.

Figure 13.– Variation with Mach number of the effects of the dive brakes.

Figure 14.– Variation with Mach number of the effects of the bomb bay.

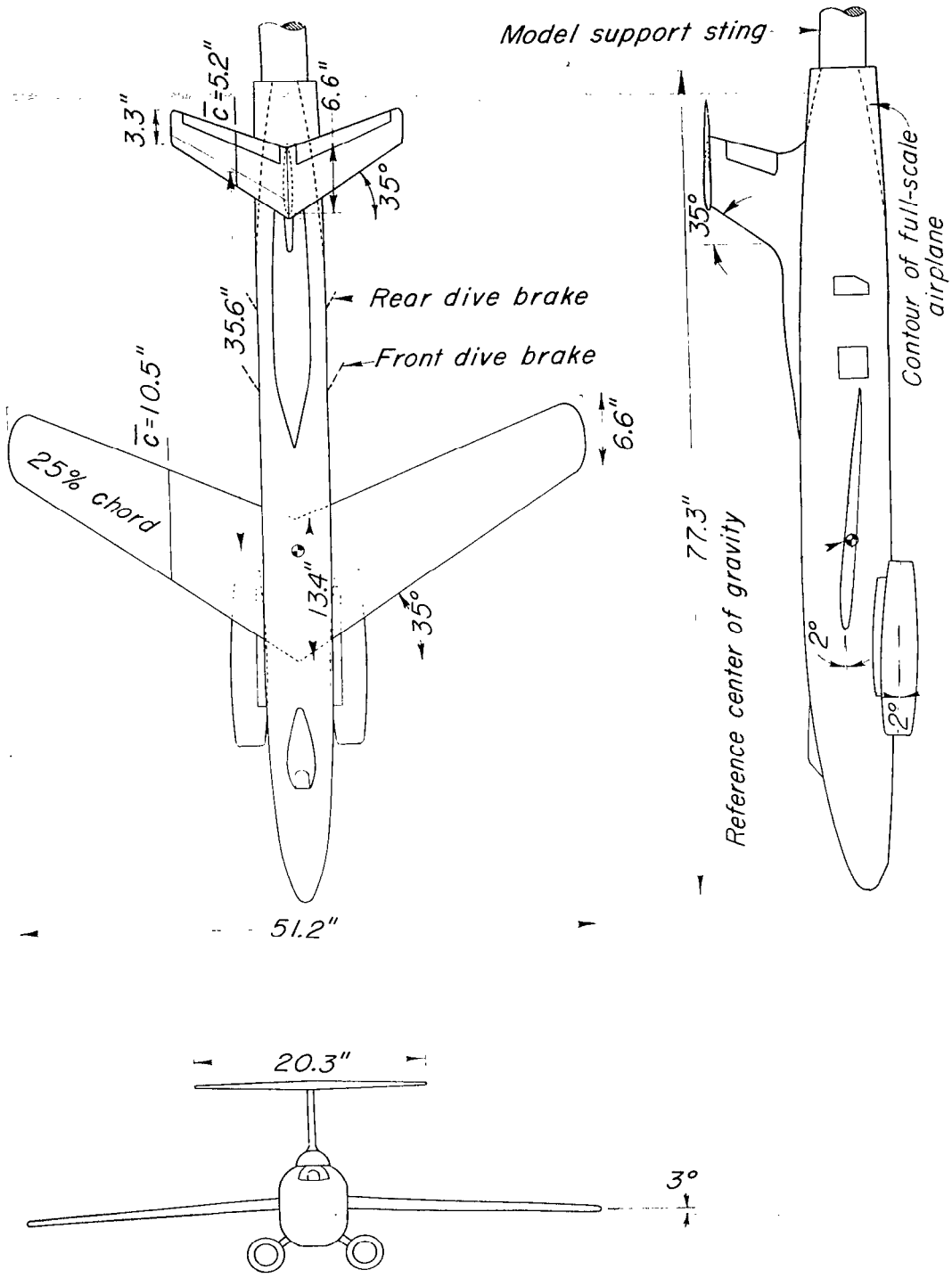

Figure 1.— Three-view drawing of 0.08-scale model of the Martin XB-51 airplane.

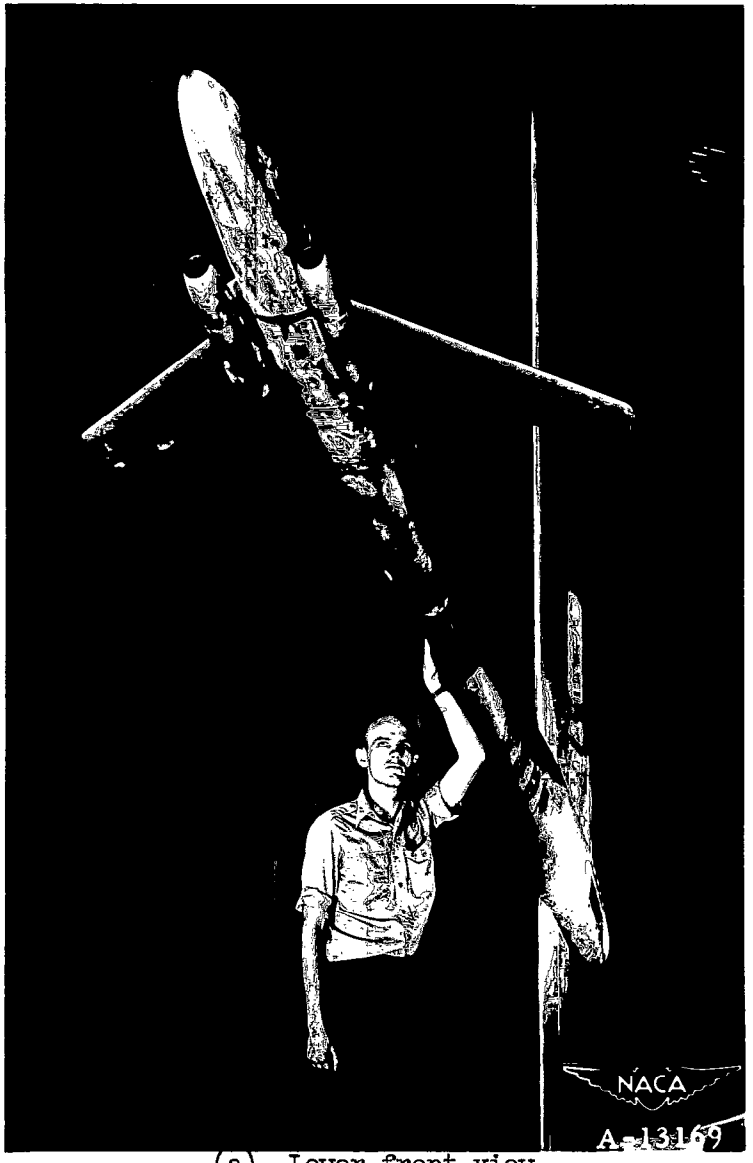

(a) Lower front view

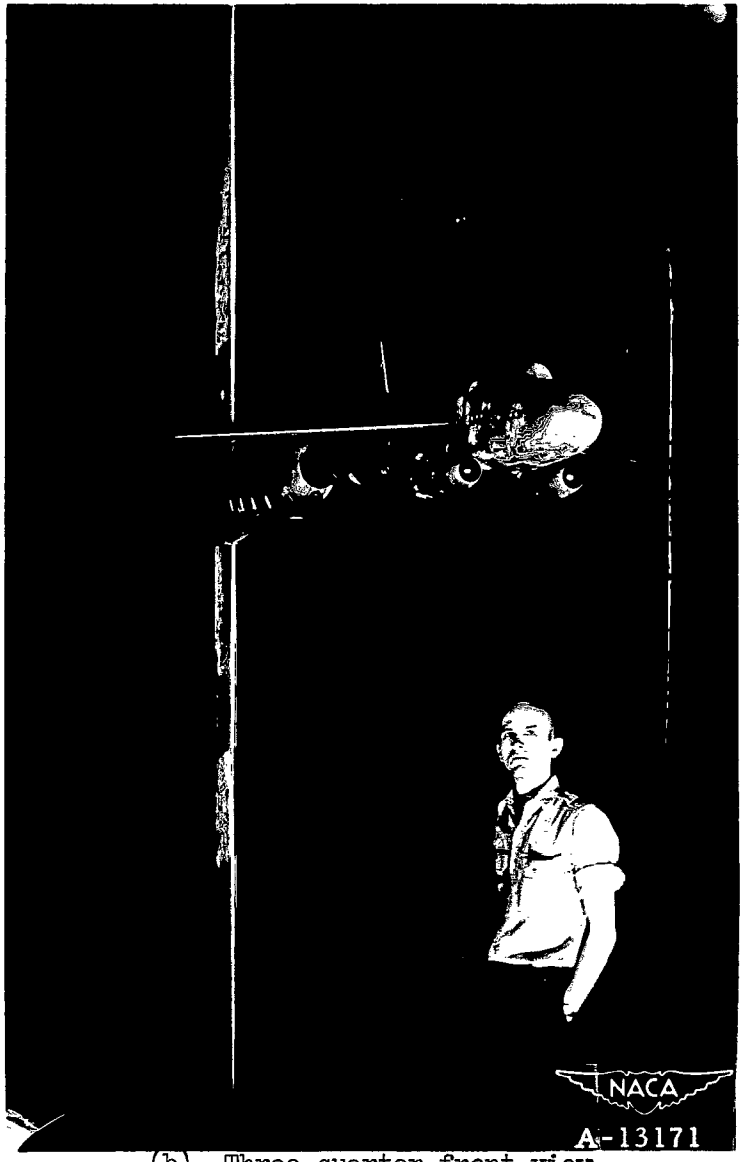

(b) Three-quarter front view

Figure 2.- The 0.08-scale model of the XB-51 airplane mounted in the wind tunnel.

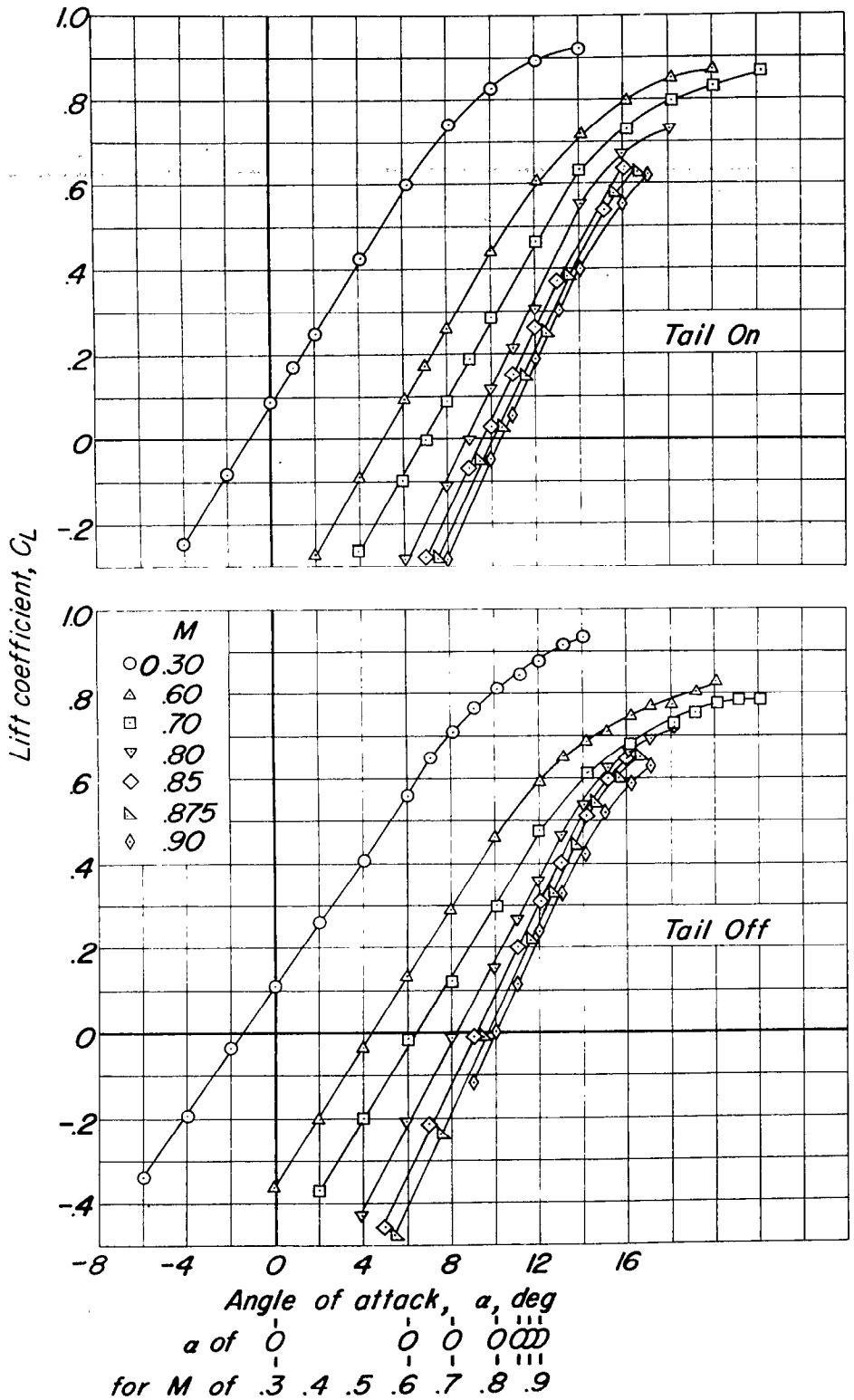

Figure 3.— Variation of lift coefficient with angle of attack at various Mach numbers

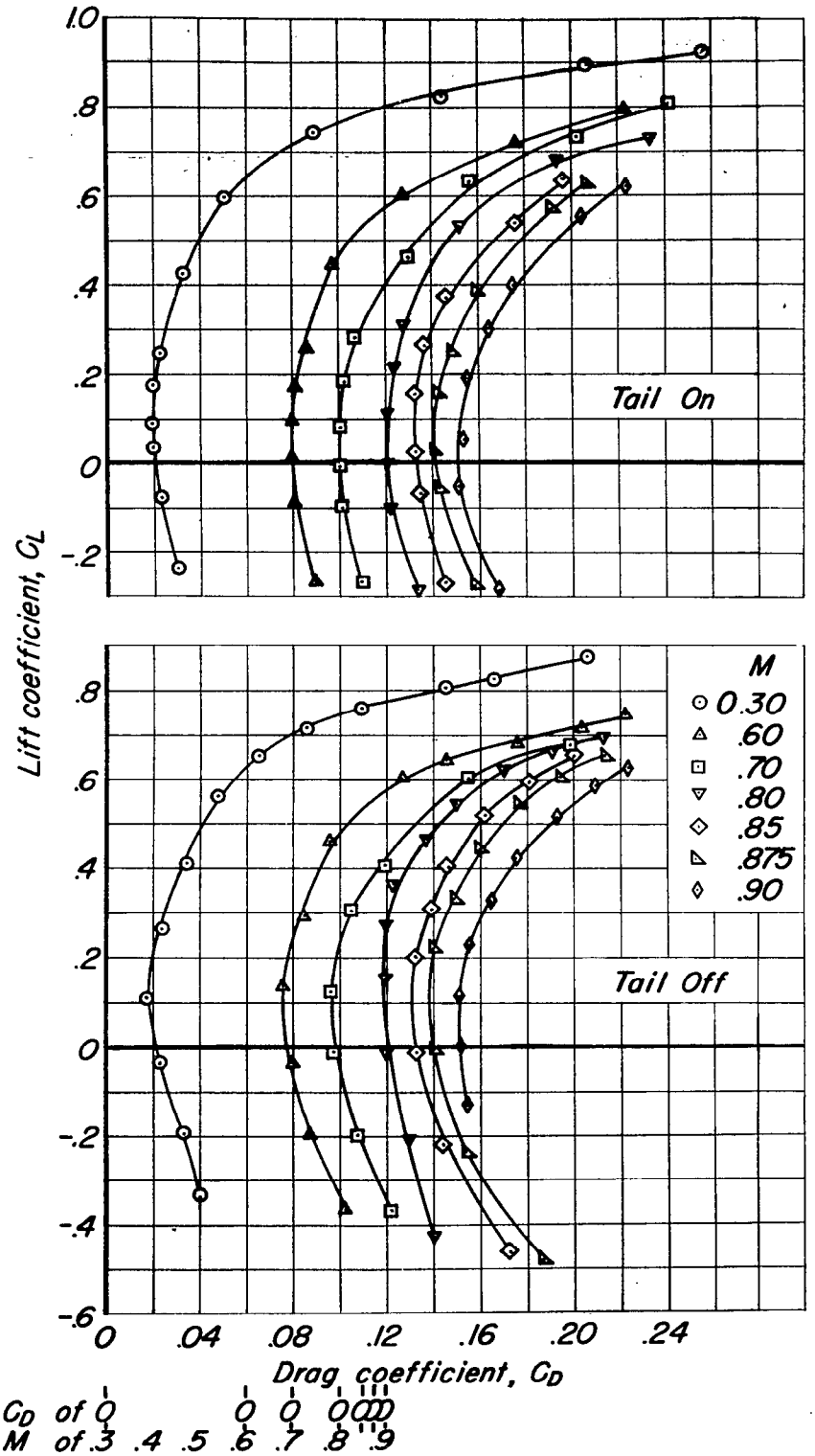

Figure 4.— Variation of lift coefficient with drag coefficient at various Mach numbers.

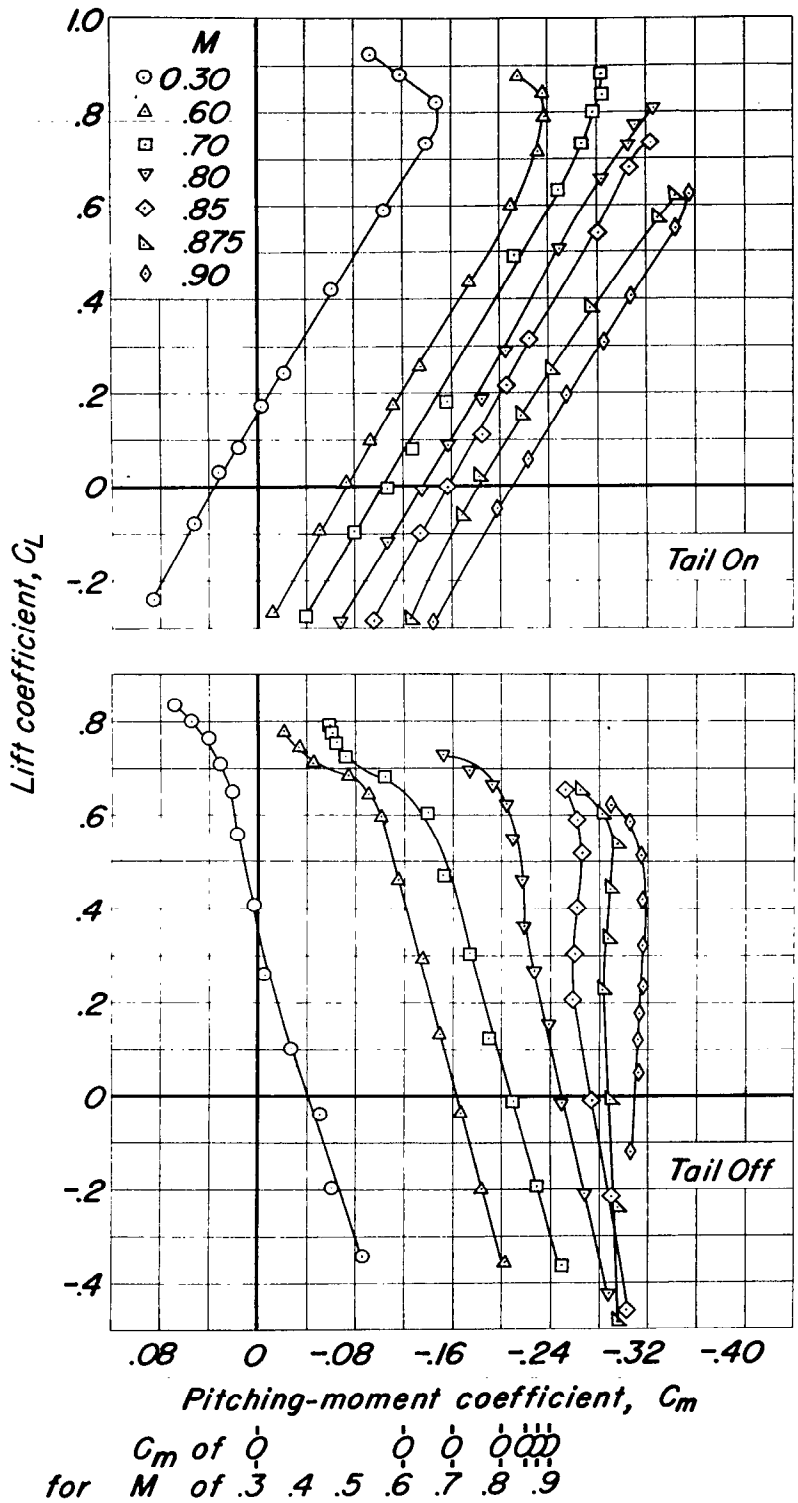

Figure 5.—Variation of lift coefficient with pitching-moment coefficient at various Mach numbers.

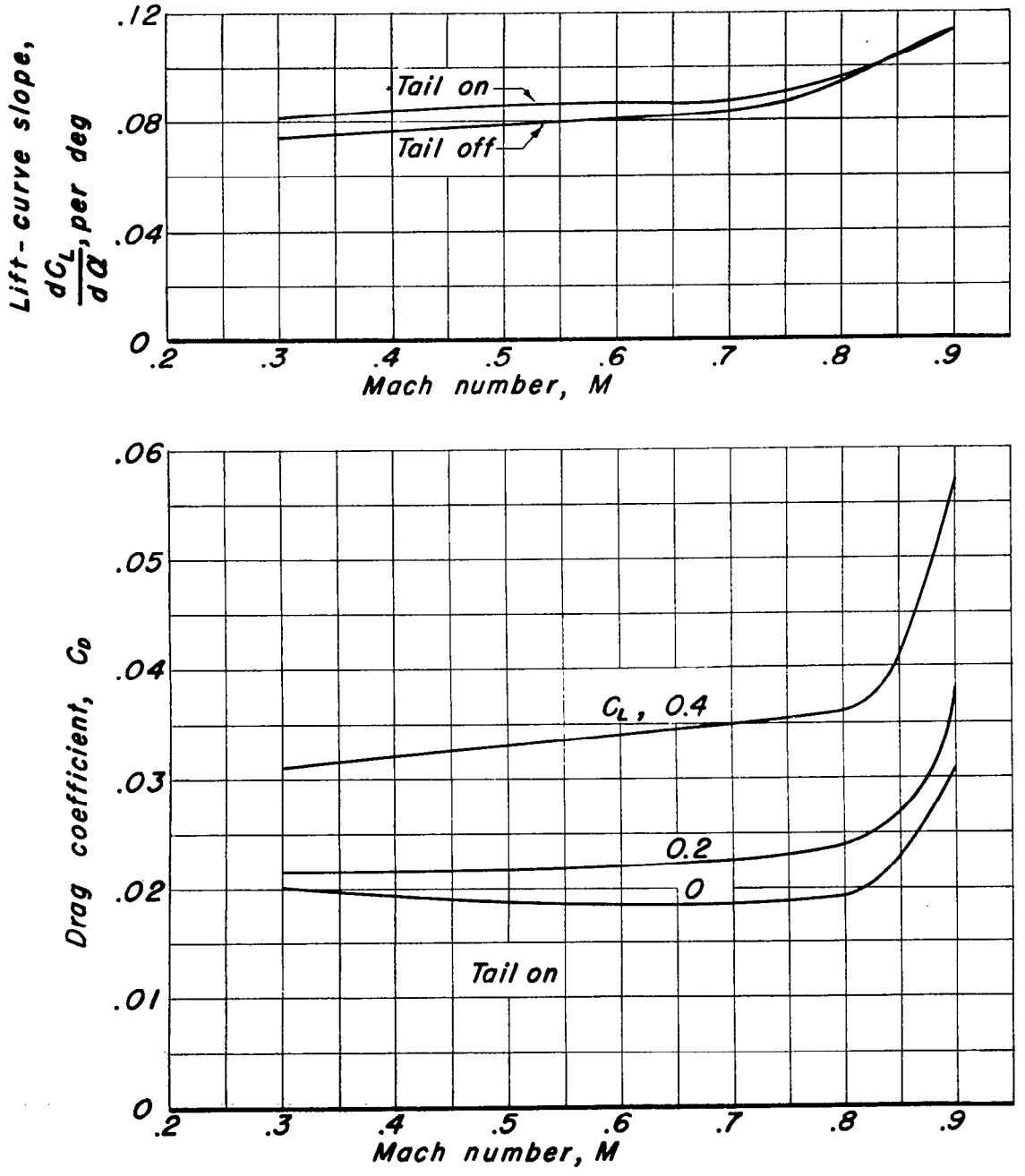

Figure 6.—Variation of lift-curve slope and drag coefficient with Mach number.

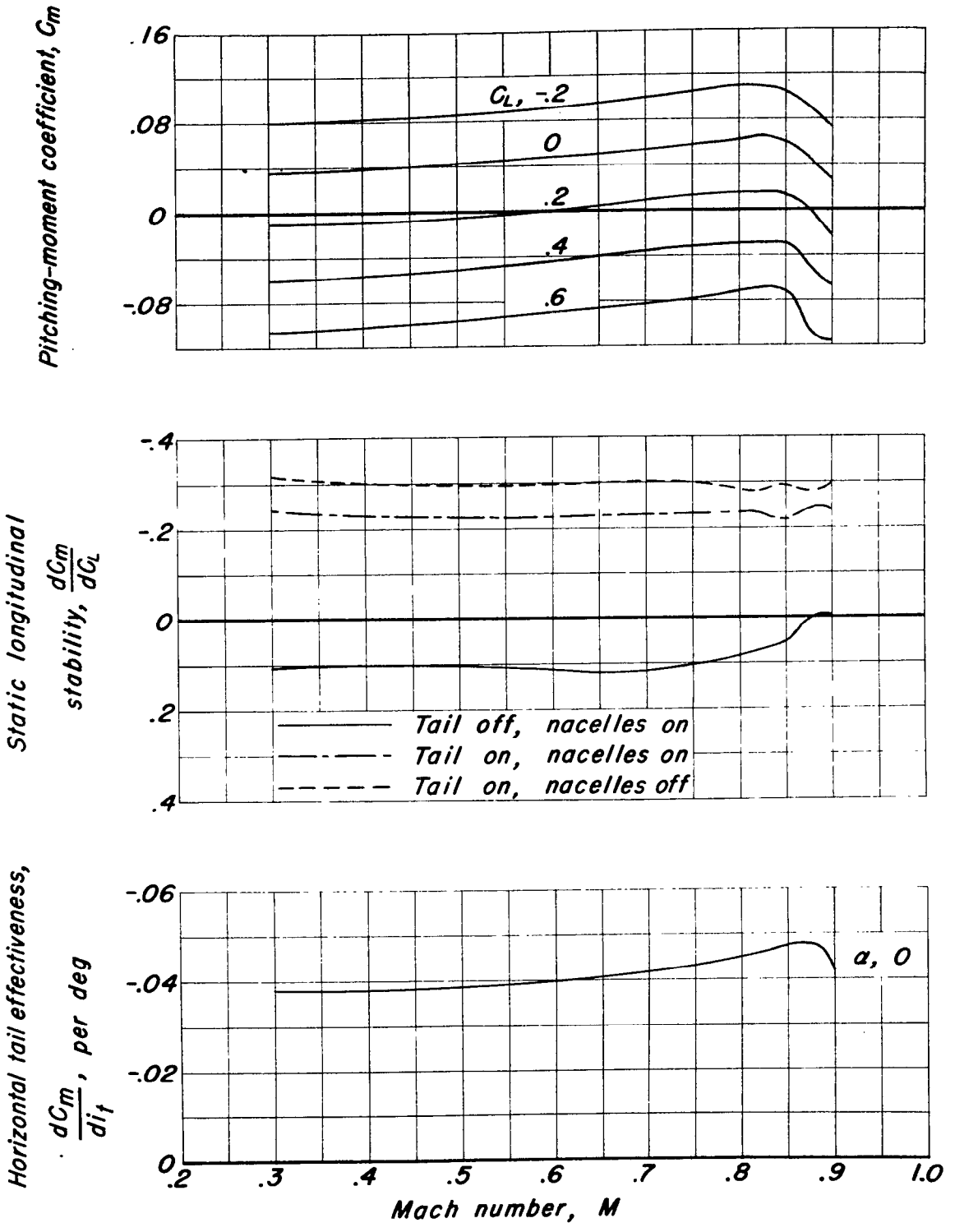

Figure 7.– Variation with Mach number of the pitching-moment coefficient, static longitudinal stability, and horizontal tail effectiveness.

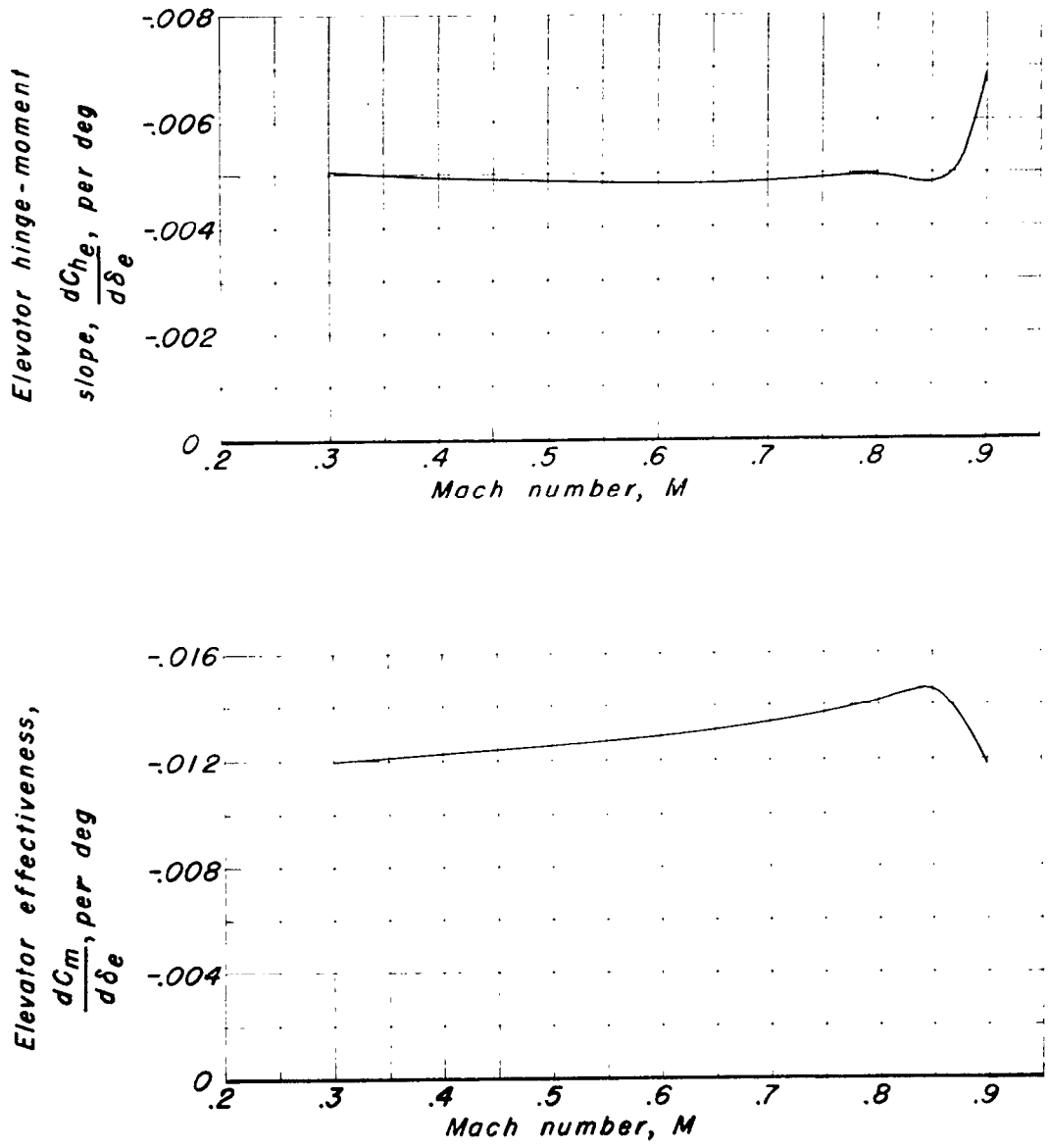

Figure 8.— Variation of elevator hinge-moment slope and effectiveness with Mach number.

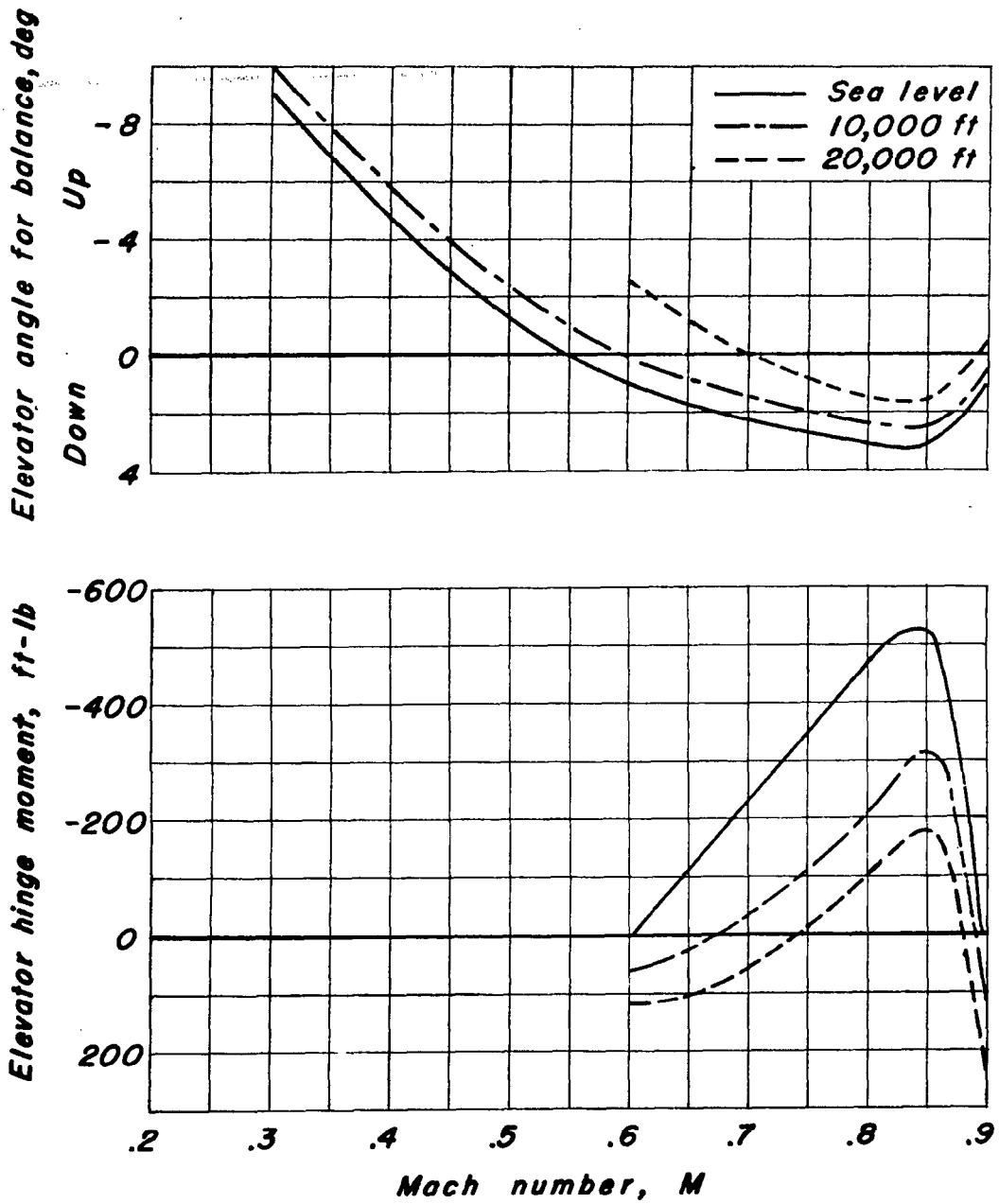

Figure 9.— Variation with Mach number of elevator angle and hinge moment at balance in level flight.

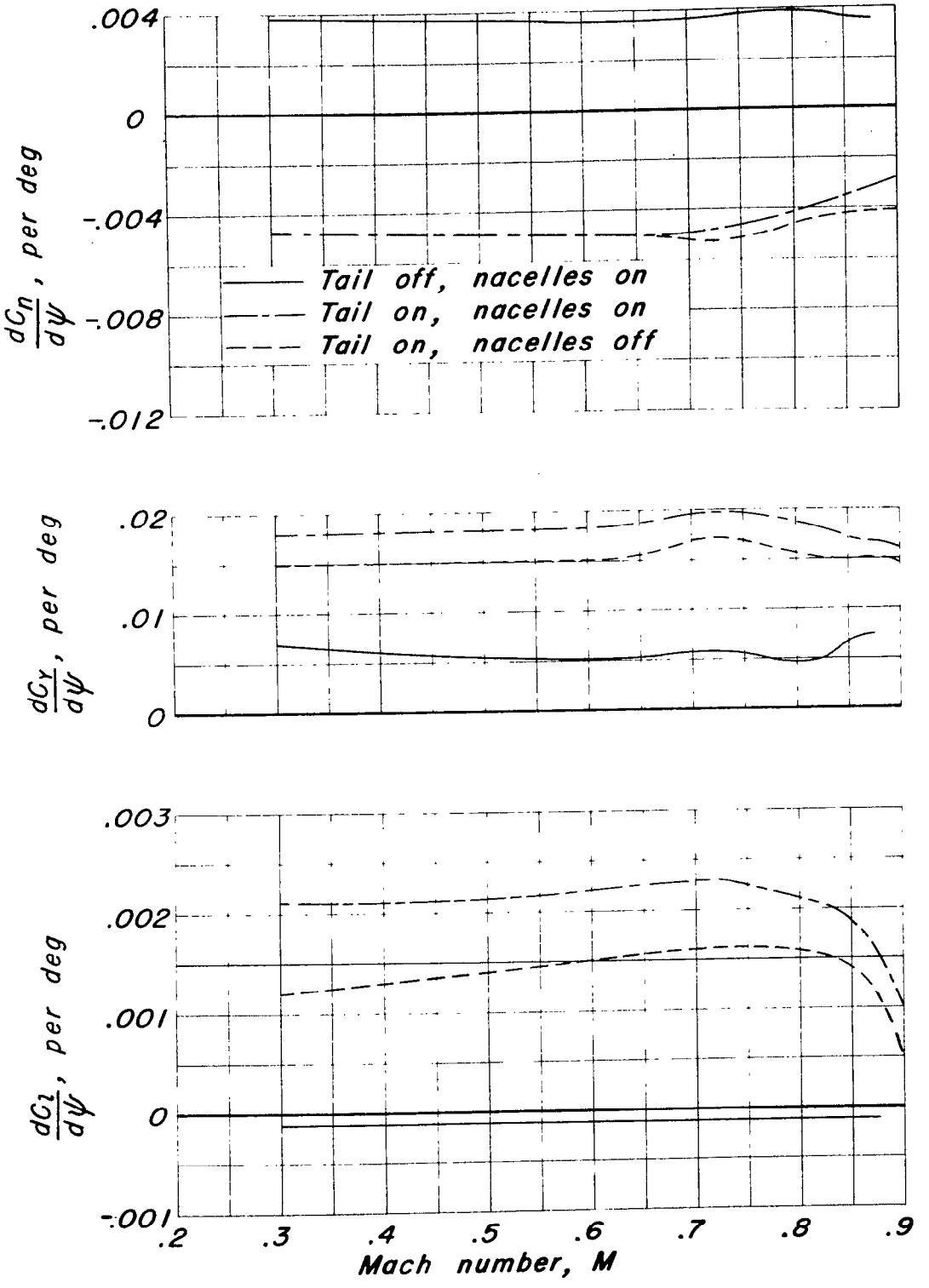

Figure 10.— Variation with Mach number of the lateral and directional characteristics.

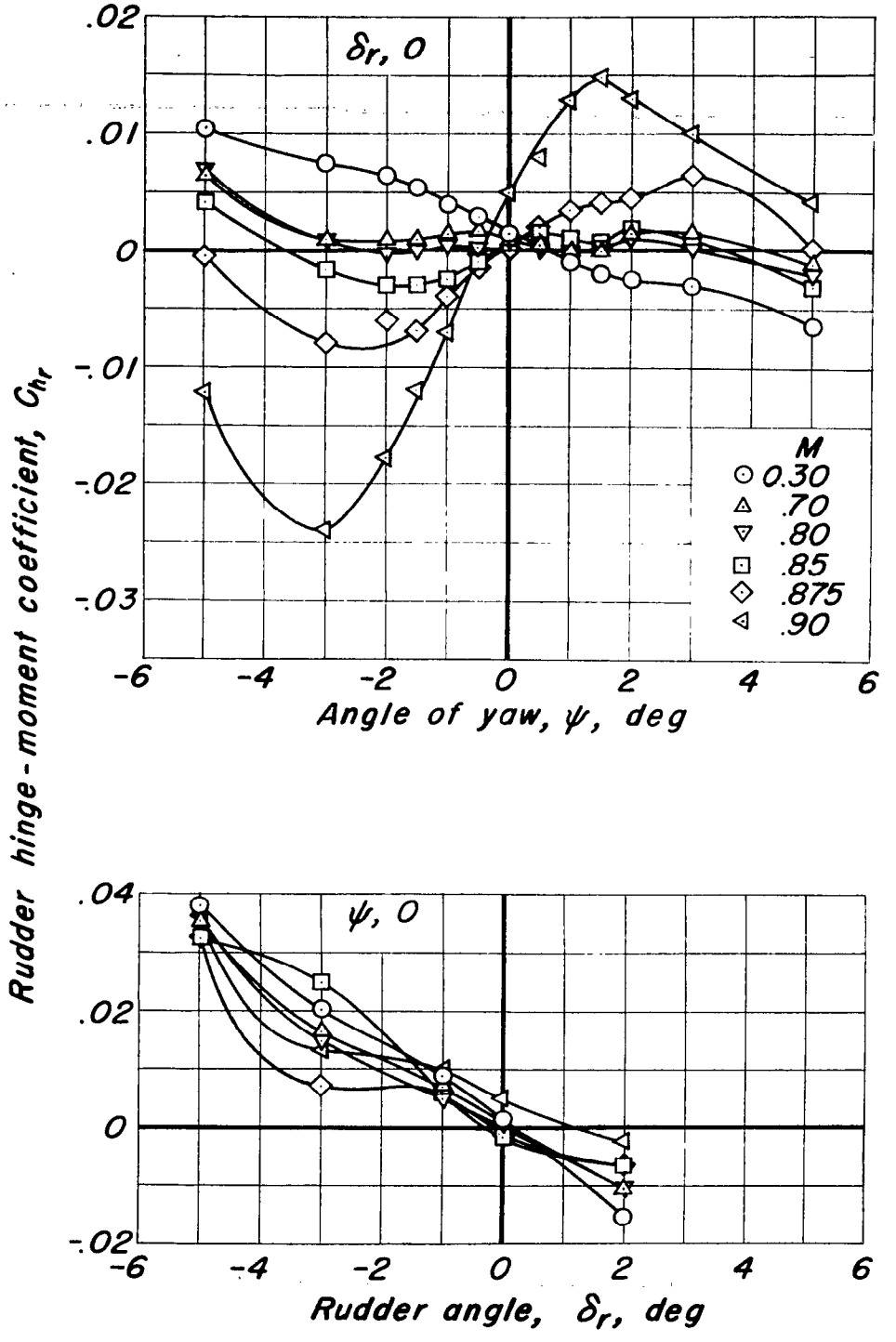

Figure 11.— Typical variations of rudder hinge-moment coefficient with angle of yaw and with rudder angle.

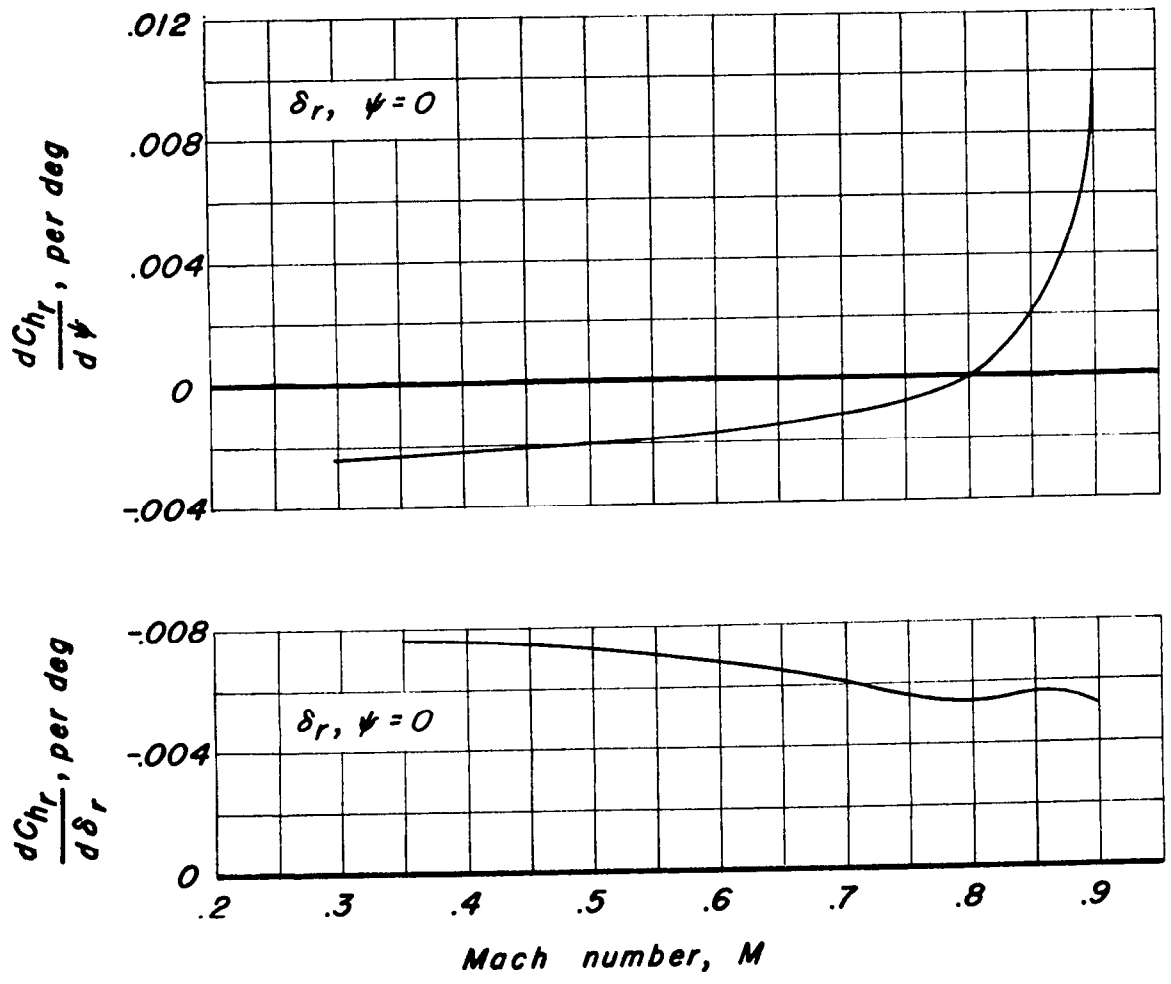

Figure 12.— Variation of rudder hinge-moment characteristics with Mach number.

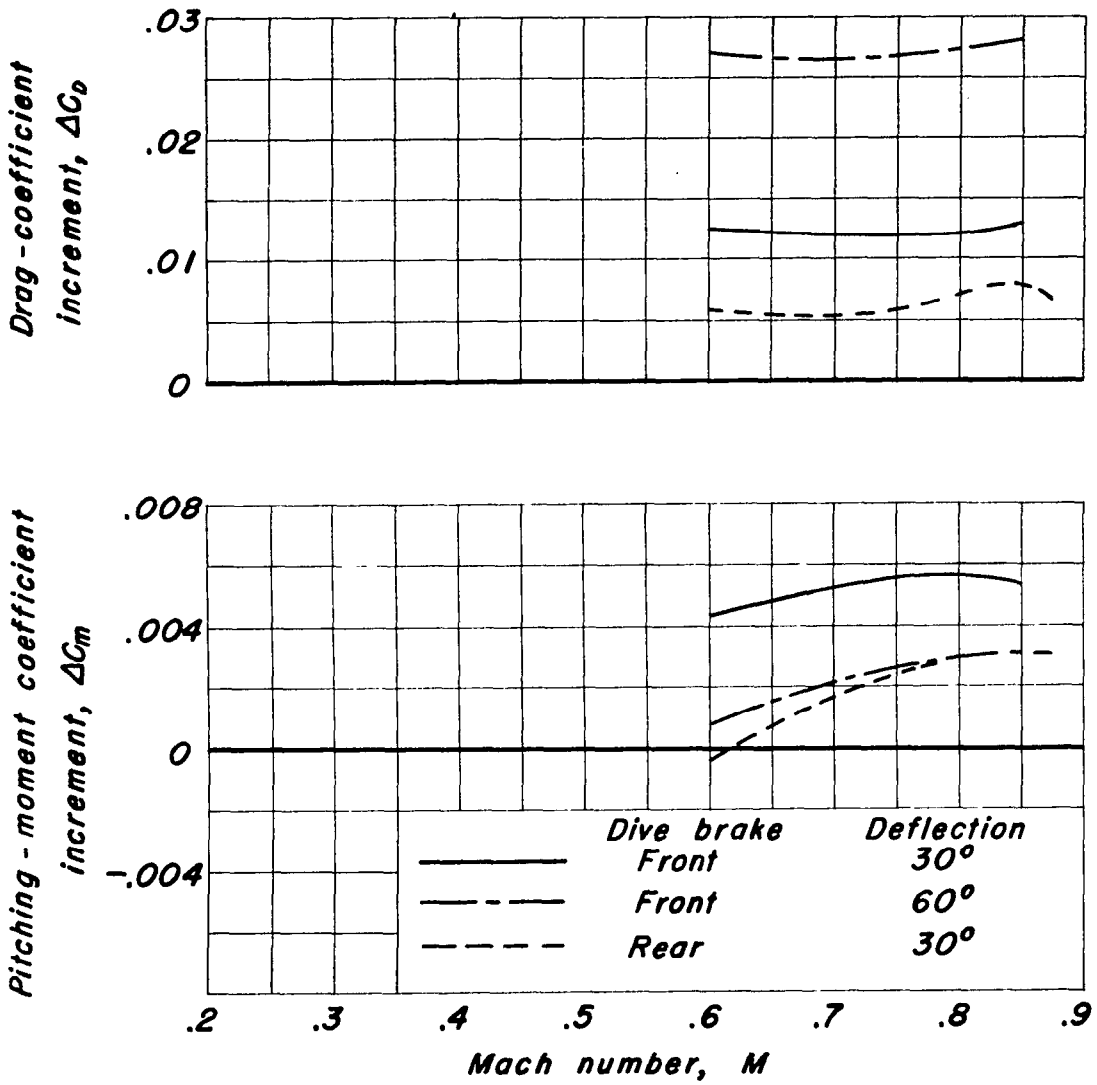

Figure 13.— Variation with Mach number of the effects of the dive brakes.

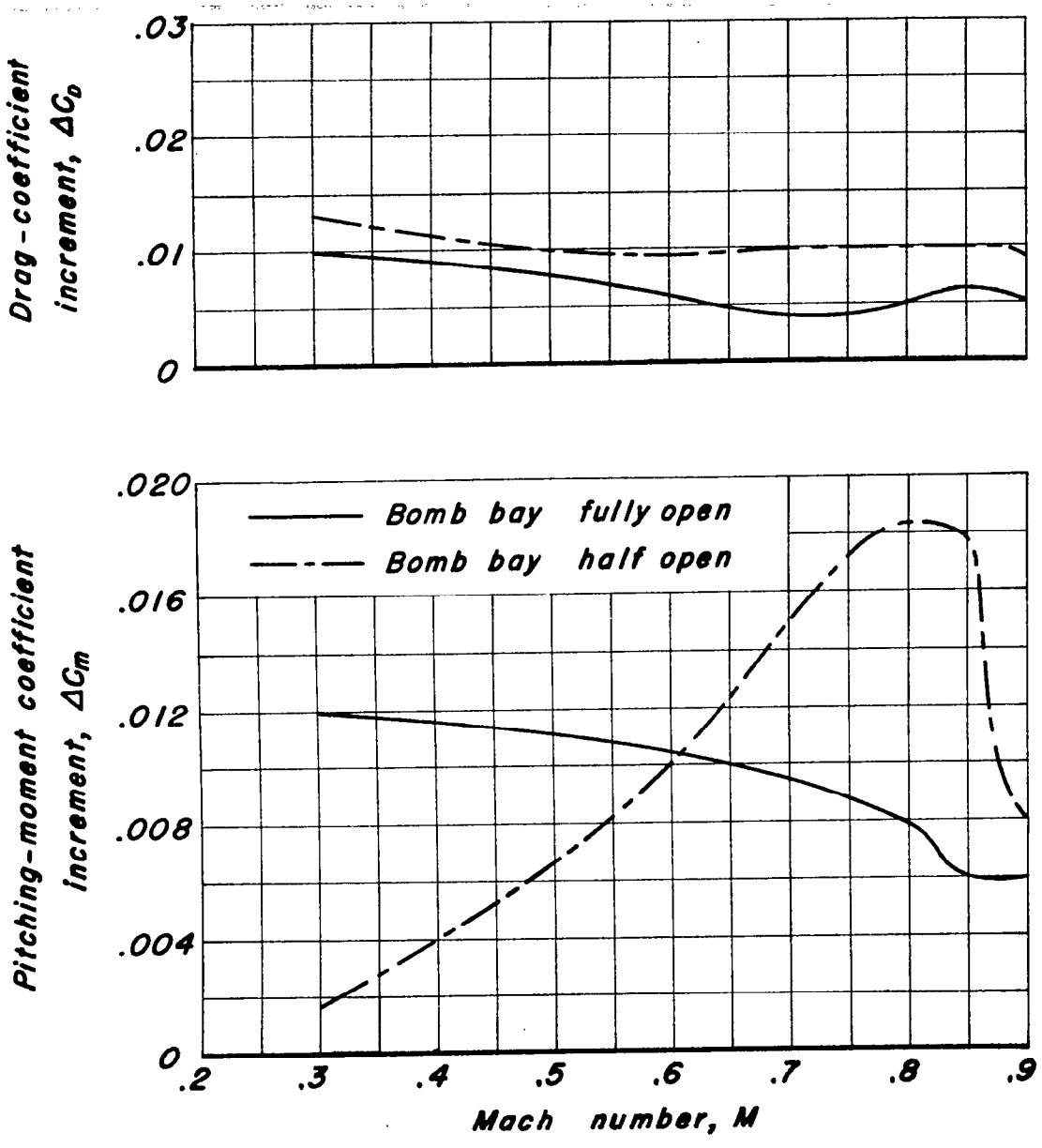

Figure 14.— Variation with Mach number of the effects of the bomb bay.